Cu - O - Cu superexchange of some polyolate-bridged copper(II) clusters

1996 J. Phys.: Condens. Matter 8 1539

(http://iopscience.iop.org/0953-8984/8/10/024)

J. Phys.: Condens. Matter **8** (1996) 1539–1555. Printed in the UK

Cu–O–Cu superexchange of some polyolate-bridged copper(II) clusters

Bernd Pilawa†§ and Jörg Schuhmacher‡

† Physikalisches Institut, Universität Karlsruhe (TH), POB 6980, D-76128 Karlsruhe, Germany
‡ Institut für Anorganische Chemie, Universität Karlsruhe (TH), POB 6980, D-76128 Karlsruhe, Germany

Received 24 July 1995, in final form 17 November 1995

Abstract. The magnetic properties of two tris-{μ-propanetriolato(3-)} tricuprate clusters: $Li_3[Cu_3(\mu\text{-}C_3H_5O_3)_3]\cdot 18H_2O$ (**1**) and $Na_3[Cu_3(\mu\text{-}C_3H_5O_3)_3]\cdot 9H_2O$ (**2**); and of a polyolato metallate cluster of sixteen Cu^{2+} ions: $Li_8[Cu_{16}(C_6H_8O_6)_4(C_6H_{10}O_6)_4]\cdot 44H_2O$ (**3**) are investigated. The Cu–O–Cu intracluster superexchange constants determined by measurements of the magnetic susceptibility are antiferromagnetic. They depend strongly on the corresponding Cu–O–Cu bonding angle and take values up to 400 cm^{-1}. The interplay of exchange narrowing and dipolar, hyperfine and g-anisotropy broadening for clusters of strongly exchange coupled Cu^{2+} ions is studied using electron spin resonance (ESR) at 9.5 GHz and 245 GHz.

1. Introduction

The structural and magnetic properties of many di-μ-hydroxo-copper(II) as well as di-μ-alkoxo-copper(II) dimers have been investigated, in order to clarify the Cu–O–Cu exchange interaction between Cu^{2+} ions [1, 2, 3]. Van Crawford *et al* [1] found that the exchange interaction correlates linearly with the Cu–O–Cu angle for hydroxo-bridged copper(II) dimers, whereas Mikuriya *et al* [4] pointed out that the planarity around the bridging oxygen atom is important for the more complicated correlation between the geometrical structure and the Cu–O–Cu exchange of alkoxo-bridged copper(II) dimers. Recently, Klüfers and co-workers succeeded in crystallizing polyolate-bridged clusters of three Cu^{2+} ions: $Li_3[Cu_3(\mu\text{-}C_3H_5O_3)_3]\cdot 18H_2O$ (**1**) [5, 6] and $Na_3[Cu_3(\mu\text{-}C_3H_5O_3)_3]\cdot 9H_2O$ (**2**) [7]; and one cluster of sixteen Cu^{2+} ions: $Li_8[Cu_{16}(C_6H_8O_6)_4(C_6H_{10}O_6)_4]\cdot 44H_2O$ (**3**) [8]. Since each of the cluster compounds is crystallographically characterized, we measured the magnetic susceptibility and determined the correlation between the Cu–O–Cu angle and the corresponding exchange constants.

An electron spin-resonance (ESR) investigation of compound (**2**) was carried out, in order to study the connection between the spin-density distribution of the cluster and the ESR linewidth and g-factors. Since the spin-density distribution on the cluster can be determined from susceptibility measurements, a comparison between experimental results and calculations based on crystallographic properties and a well known molecular spin-density distribution is possible. We report on ESR measurements at a frequency of 9.5 GHz and preliminary measurements at 245 GHz, which show that resonances of magnetically inequivalent clusters can be decoupled, so more detailed information on the ground-state

§ Present address: LCMI-CNRS, BP 166, 38042 Grenoble Cédex 9, France.

0953-8984/96/101539+17$19.50

properties of individual clusters is obtainable from the angular variation of the resolved resonance signals.

2. Crystallographic and experimental details

The Cu^{2+} clusters $Li_3[Cu_3(\mu\text{-}C_3H_5O_3)_3]\cdot 18H_2O$ (**1**), $Na_3[Cu_3(\mu\text{-}C_3H_5O_3)_3]\cdot 9H_2O$ (**2**), and $Li_8[Cu_{16}(C_6H_8O_6)_4(C_6H_{10}O_6)_4]\cdot 44H_2O$ (**3**) have in common that the Cu^{2+} ions are bridged by fully or partially deprotonated polyols. While the tricuprate clusters of (**1**) and (**2**) are formed with triply deprotonated glycerol as ligands [5], the clusters of (**3**) are composed of completely as well as partially deprotonated sorbitol ligands [8]. (**1**) and (**2**) crystallize in hexagonal structures, and (**3**) crystallizes in a monoclinic lattice structure. The clusters are separated and surrounded by the cations and water molecules. Table 1 compares the lattice parameters and space groups of the three compounds.

Table 1. Results of the x-ray diffraction analysis taken from [5] for compound (**1**), [7] for compound (**2**) and [8] for compound (**3**).

	(**1**)	(**2**)	(**3**)
Formula	$Li_3[Cu_3(\mu\text{-}C_3H_5O_3)_3]\cdot 18H_2O$	$Na_3[Cu_3(\mu\text{-}C_3H_5O_3)_3]\cdot 9H_2O$	$Li_8[Cu_{16}(C_6H_8O_6)_4(C_6H_{10}O_6)_4]\cdot 44H_2O$
Mass (g mol^{-1})	820.96	688.96	3318.03
Space group	$P\bar{3}c1$	$P\bar{6}2c$	$P2_1$
a (Å)	12.788	14.748	17.489
b (Å)	12.788	14.748	16.394
c (Å)	24.205	20.138	21.255
α	90°	90°	90°
β	90°	90°	100.75°
γ	120°	120°	90°
V (Å^3)	3428	3793	5988

The central part of each of the $[Cu_3(\mu\text{-}C_3H_5O_3)_3]$ clusters is formed of a hexagon of copper and oxygen atoms. The point symmetries of the clusters of (**1**) and (**2**) are C_3 and C_s, respectively. For the clusters (**1**) all of the Cu–O–Cu angles important for the superexchange interaction are equal and Klaassen and Klüfers [5] determined an angle of 120.8°. For the clusters of the compound (**2**) there are two different Cu–O–Cu angles. When Cu_1, Cu_2 and Cu_3 denote copper ions above, below and on the mirror plane, the angle Cu_1–O–Cu_2 is 145°, and the angle Cu_1–O–Cu_3 is 125°. Figure 1 displays the positions of the $[Cu_3(\mu\text{-}C_3H_5O_3)_3]$ clusters within the elementary cell of compound (**2**).

The sixteen Cu^{2+} ions of the clusters (**3**) form a torus of approximately D_2 symmetry. There are two groups of five Cu^{2+} ions for which the Cu–O–Cu angles are about 138°, and two groups of three Cu^{2+} ions for which the Cu–O–Cu angles are about 130°. These four groups are linked by Cu–O–Cu bonds at angles of about 116° [8].

The static magnetic susceptibility was determined using a commercial SQUID magnetometer (Quantum Design MPMS) between 2 and 300 K in a magnetic field of 20 kOe. During the measurement, the sample consisting of many single crystals was surrounded by a low-pressure helium atmosphere. The sample masses were 29 mg for (**1**), 9 mg for (**2**) and 15 mg for (**3**).

X-band ESR (9.5 GHz) was recorded with a Bruker ESP300E spectrometer equipped with an Oxford ESR900 cryostat. Measurements for various single crystals ($\simeq 1\times 1\times 1$ mm^3) were made.

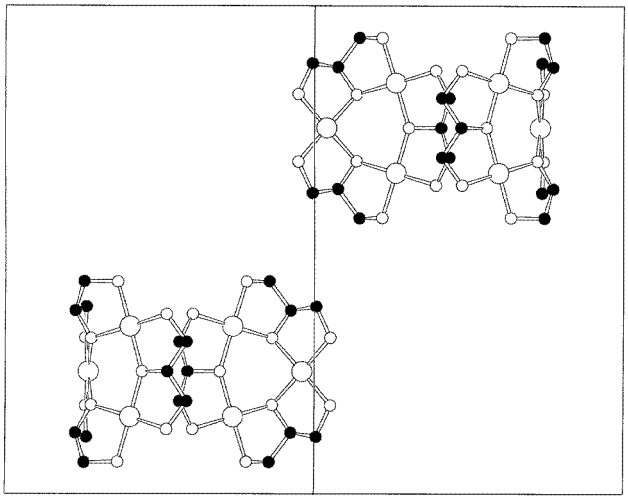

(*a*)

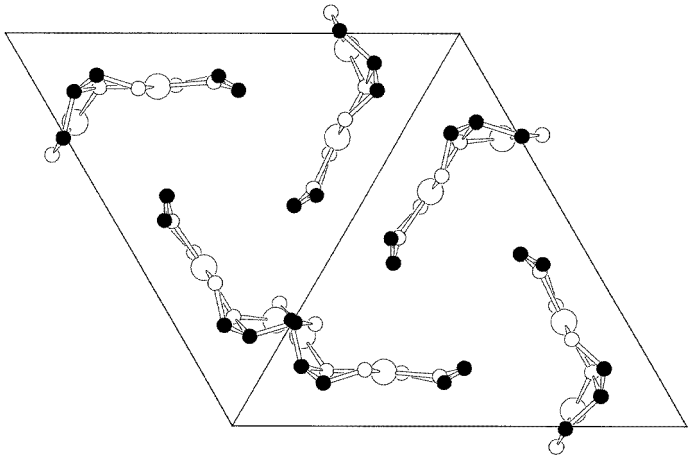

(*b*)

Figure 1. The unit cell of (**2**). Black dots: carbon; small circles: oxygen; large circles: copper. (*a*) The view along [110]. (*b*) The view along [001].

ESR at 245 GHz was measured at the Laboratoire Des Champs Magnétiques Intenses in Grenoble [9].

3. Magnetic susceptibility

*3.1. The magnetic susceptibility of $Li_3[Cu_3(\mu\text{-}C_3H_5O_3)_3]\cdot 18H_2O$ (**1**) and $Na_3[Cu_3(\mu\text{-}C_3H_5O_3)_3]\cdot 9H_2O$ (**2**)*

The static magnetic susceptibilities χ and χT of compounds (**1**) and (**2**) for temperatures between 2 and 300 K are shown in figures 2 and 3, respectively. Although the temperature dependence of χ seems to follow a Curie–Weiss law, χT reveals a more complicated

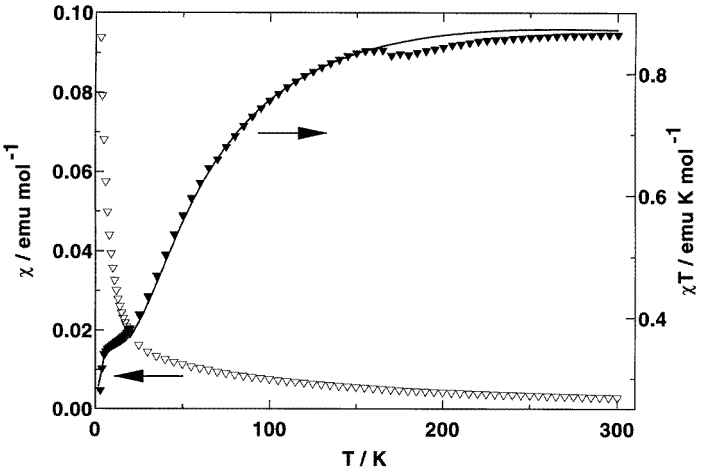

Figure 2. The magnetic susceptibility χ (open triangles) and χT (full triangles) of (**1**). The solid line was calculated using equation (5). The origin of the small anomaly at about 170 K is not clear since specific heat measurements show no anomaly in this temperature region.

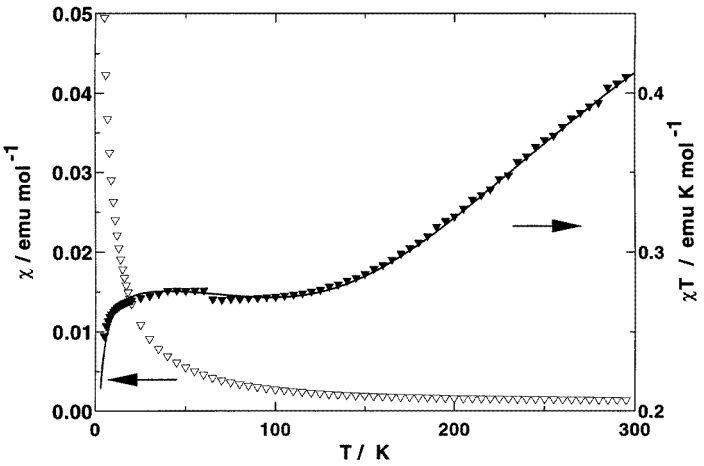

Figure 3. The magnetic susceptibility χ (open triangles) and χT (full triangles) of (**2**). The solid line was calculated using equation (6). The small jump at about 60 K for χT originates presumably from oxygen condensed into the sample chamber.

structure. When the temperature is increased, χT rises from small values at 2 K to a plateau at $\chi T \simeq 0.3$ emu K mol^{-1} and increases further until finally a second plateau is reached at values of $\chi T \simeq 0.9$ emu K mol^{-1}. Qualitatively, this result can be interpreted in the following way. The copper ions are strongly antiferromagnetically coupled within the clusters. Therefore the ground state is a doublet with the effective spin $s = 1/2$ and the Curie constant $C = 0.374$ emu K mol^{-1}. The susceptibility corresponding to three copper $s = 1/2$ spins is observable only for temperatures which are large compared with the antiferromagnetic intracluster exchange. The decrease of χT below $\simeq$0.3 emu K mol^{-1} at low temperatures reveals a weak antiferromagnetic intercluster interaction.

Our quantitative analysis of the magnetic susceptibility starts from the paramagnetic susceptibility of isolated clusters of three $s = 1/2$ spins, coupled according to the Heisenberg exchange Hamiltonian

$$H = -\sum_{i=1}^{3} J_i \boldsymbol{S}_i \cdot \boldsymbol{S}_{i+1} \qquad \text{with } \boldsymbol{S}_1 = \boldsymbol{S}_4. \tag{1}$$

For three $s = 1/2$ spins, there are two doublet states $|S = 1/2, \alpha\rangle$ and $|S = 1/2, \beta\rangle$ and a quartet state $|S = 3/2\rangle$. Their energies are

$$E_{1/2,\substack{\alpha\\\beta}} = \tfrac{1}{4}(J_1 + J_2 + J_3) \pm \lambda \qquad E_{3/2} = -\tfrac{1}{4}(J_1 + J_2 + J_3)$$

respectively. λ is given by

$$\lambda = +\sqrt{K^2 + \Delta^2}$$

with

$$K = -J_1/2 + J_2/4 + J_3/4 \qquad \Delta = (\sqrt{3}/4)(J_3 - J_2).$$

Since for a magnetic field of 20 kOe the magnetic energy is very much smaller than the intracluster exchange and thermal energies at the temperatures of interest, the magnetic susceptibilities of the clusters are calculated in the zero-magnetic-field approximation. For compound (**1**), due to its high symmetry (C_3), all of the exchange constants for exchange between the Cu^{2+} ions of the clusters are equal ($J_1 = J_2 = J_3 = J$) and the magnetic susceptibility is given by

$$\chi = \frac{C}{T}\left\{\frac{1 + 5\mathrm{e}^{3J/2k_BT}}{1 + \mathrm{e}^{3J/2k_BT}}\right\} \tag{2}$$

where $C = N_A g^2 \mu_B^2 s(s+1)/3k_B$ is the Curie constant, N_A is Avogadro's number, μ_B is the Bohr magneton, k_B is the Boltzmann constant, $g = 2$ and $s = 1/2$.

Due to the C_s symmetry of the clusters of the compound (**2**), only two of the exchange constants are equal: $J_1 \neq J_2 = J_3$, and the magnetic susceptibility becomes

$$\chi = \frac{C}{T}\left\{\frac{1 + \mathrm{e}^{(J_2 - J_1)/k_BT} + 10\mathrm{e}^{3J_2/2k_BT}}{1 + \mathrm{e}^{(J_2 - J_1)/k_BT} + 2\mathrm{e}^{3J_2/2k_BT}}\right\}. \tag{3}$$

In order to achieve a spin-$s = 1/2$ ground state of the cluster of (**2**), at least the exchange constant J_2 has to be negative. Then both equation (2) and equation (3) show the expected behaviour: $\chi = C/T$ at low temperatures and $\chi = 3C/T$ at high temperatures. Due to there being two possible doublet ground states ($|S = 1/2, \alpha\rangle$ or $|S = 1/2, \beta\rangle$) for the cluster (**2**), there are two different sets of exchange constants leading to the same paramagnetic susceptibility. They are connected according to

$$\tilde{J}_1 = \frac{1}{3}(-J_1 + 4J_2) \qquad \tilde{J}_2 = \frac{1}{3}(2J_1 + J_2). \tag{4}$$

For an analysis of the experimental data, two further points have to be considered. First, at low temperatures the antiferromagnetic intercluster interaction is important and a Curie–Weiss temperature has to be included in equations (2) and (3). Second, at temperatures above 50 K, the paramagnetic contribution to the magnetic moment of the sample becomes very small and the diamagnetism of the sample cannot be neglected. Taking into account these considerations, χT of compound (**1**) is approximated by

$$\chi T = \frac{C}{1 - \Theta/T}\left\{\frac{1 + 5\mathrm{e}^{3J/2k_BT}}{1 + \mathrm{e}^{3J/2k_BT}}\right\} + \chi_{Dia} T \tag{5}$$

and χT of compound (**2**) by

$$\chi T = \frac{C}{1-\Theta/T}\left\{\frac{1+\mathrm{e}^{(J_2-J_1)/k_BT}+10\mathrm{e}^{3J_2/2k_BT}}{1+\mathrm{e}^{(J_2-J_1)/k_BT}+2\mathrm{e}^{3J_2/2k_BT}}\right\}+\chi_{Dia}T. \tag{6}$$

The diamagnetic susceptibility χ_{Dia} of (**1**) and (**2**) can be estimated. With the susceptibilities of Cu^{2+}: -11×10^{-6} emu mol^{-1}; Li^+: -0.6×10^{-6} emu mol^{-1}; Na^+: -5×10^{-6} emu mol^{-1} [10]; $C_3H_8O_3$: -57×10^{-6} emu mol^{-1}; and H_2O: -13×10^{-6} emu mol^{-1} [11]; one gets for compound (**1**) $\chi_{Dia}=-440\times10^{-6}$ emu mol^{-1} and for (**2**) $\chi_{Dia}=-336\times10^{-6}$ emu mol^{-1}.

A fit of equation (5) to the experimentally determined χT-values of compound (**1**) yields for the exchange constant $J/hc=-42\pm2$ cm^{-1} and for the Curie–Weiss temperature $\Theta=-0.6\pm0.1$ K (the solid line in figure 2). The Curie constant was fixed at 0.374 emu K mol^{-1} and χ_{Dia} at the estimated value.

Fitting equation (6) to the measurements for compound (**2**) yields $\Theta=-1.0\pm0.2$ K and two sets of exchange constants $J_1/hc=95\pm4$ cm^{-1}, $J_2/hc=-315\pm4$ cm^{-1}, or alternatively $J_1/hc=-450\pm4$ cm^{-1}, $J_2/hc=-42\pm4$ cm^{-1}. In contrast to the case for compound (**1**), it was not possible to fix the Curie constant C and the diamagnetic susceptibility χ_{Dia} to the expected values. The solid line of figure 3 was calculated with $\chi_{Dia}=-180\times10^{-6}$ emu mol^{-1} and $C=0.29$ emu K mol^{-1}. Due to the small magnetic moment of the sample for temperatures above 50 K ($<10^{-3}$ G cm^3), the small value of χ_{Dia} may be caused by a slight overcorrection of the diamagnetic contribution of the sample holder. The reduced Curie constant can stem from inclusions of diamagnetic sodium nitrate within crystals of compound (**2**), since crystals of (**2**) may grow on sodium nitrate crystals.

Comparing the results obtained for compounds (**1**) and (**2**), it becomes obvious that the exchange constants of (**2**) are $J_1/hc=-450\pm4$ cm^{-1} and $J_2/hc=-42\pm4$ cm^{-1}. First of all, the Cu–O–Cu angle of 125° for J_2 is comparable to the corresponding angle of cluster (**1**). Therefore the corresponding exchange constants should also be comparable. This choice of exchange constants is confirmed by the value of $|J_1|$, which is considerably larger than $|J_2|$ due to the larger Cu–O–Cu angle of 144° favouring an antiferromagnetic interaction.

3.2. The magnetic susceptibility of $Li_8[Cu_{16}(C_6H_8O_6)_4(C_6H_{10}O_6)_4]\cdot44H_2O$ (3)

The temperature dependence of χ and χT for compound (**3**) is shown in figure 4. Qualitatively, these results can be interpreted by considering the various Cu–O–Cu angles. Since there are two groups of copper ions with Cu–O–Cu angles of around 138° and two with angles of around 130°, one can expect the spins of each group of Cu^{2+} ions to be strongly coupled. According to the results obtained for the clusters (**1**) and (**2**), the copper–copper exchange values $|J/hc|$ should range from about 40 up to 400 cm^{-1}. Therefore, each of the four spin groups can be characterized by an effective spin $s=1/2$, for temperatures below about 50 K. However, since the four groups of copper ions are linked by exchange paths with Cu–O–Cu angles of about 115°, there is also an antiferromagnetic interaction between the effective spins $s=1/2$ of the four spin groups. Aside from possible intercluster exchange interactions, which are presumed to be very small due to the large intercluster distances [8], this exchange interaction is mostly responsible for the decrease of χT at low temperature. A fit of the Curie–Weiss law $\chi=C(T-\Theta)^{-1}+\chi_0$ (the solid line in figure 4) yields $C=1.4$ emu K mol^{-1}, $\Theta=-4.8$ K and $\chi_0=9.9\times10^{-3}$ emu mol^{-1}. The values of C and Θ confirm that at low temperatures the magnetic properties of cluster (**3**) are well described by four $s=1/2$ spins, which are weakly antiferromagnetically coupled. The small value of Θ indicates that the exchange constants for Cu–O–Cu angles of about

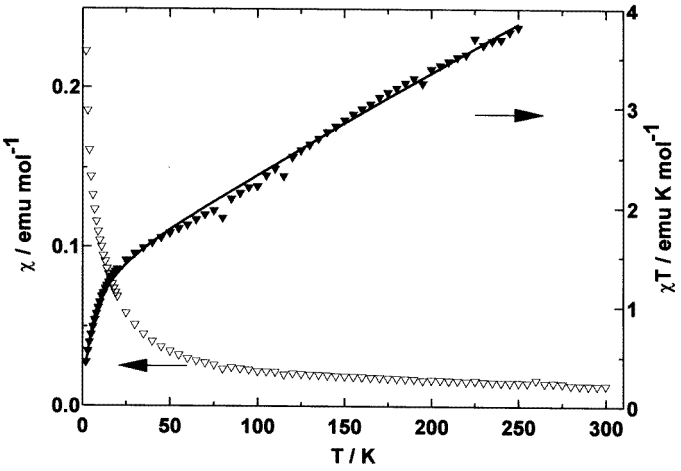

Figure 4. The magnetic susceptibility χ (open triangles) and χT (full triangles) of (**3**). The solid line shows a fit of χT (for details see the text).

116° should be in the region of a few cm^{-1}. The positive value of χ_0 is due to the linear increase of χT at higher temperatures. When the temperature is increased above 20 K, χT increases quickly above $\chi T \simeq 4C$, since, similarly to what is found for the clusters of (**1**) and (**2**), eigenstates of cluster (**3**) with larger magnetic moments can be thermally excited.

3.3. Discussion

The magnetic properties of a large number of alkoxo- and hydroxo-bridged polynuclear Cu^{2+} complexes have been determined in order to study the exchange interaction between Cu^{2+} ions [1–4]. The constants J/hc for the Cu–O–Cu superexchange range from ferromagnetic interactions with values up to 87 cm^{-1} [1] to strong antiferromagnetic interactions with values up to 700 cm^{-1} [12]. For the hydroxo-bridged Cu^{2+} dimers it was found that the exchange interaction correlates linearly with the Cu–O–Cu angle [1], whereas for the alkoxo-bridged Cu^{2+} complexes the planarity around the bridging oxygen ion is even more important than the Cu–O–Cu angle [3, 4].

For the polyolate-bridged complexes the following dependence of the Cu–O–Cu superexchange on the corresponding Cu–O–Cu angle α can be established from the analysis of the magnetic susceptibility of compounds (**1**), (**2**) and (**3**): $J/hc \simeq -450$ cm^{-1} for $\alpha \simeq 140°$, $J/hc \simeq -42$ cm^{-1} for $\alpha \simeq 123°$ and $|J/hc| < 2$ cm^{-1} for $\alpha \simeq 115°$. In contrast to the case for the hydroxo-bridged clusters the exchange interaction depends strongly on the Cu–O–Cu angle, and the change from an antiferromagnetic to a ferromagnetic behaviour occurs for the polyolate-bridged clusters for a larger Cu–O–Cu angle ($\alpha \simeq 115°$) than for the hydroxo-bridged clusters ($\alpha \simeq 99°$). These results may indicate that the planarity around the bridging oxygen ion is also important for the exchange interaction of the polyolate-bridged clusters. The coordination geometry around the bridging oxygen ion for the exchange path with the large exchange constant of cluster (**2**) is nearly planar (see figure 1), whereas the sum of bonding angles around the bridging oxygen for the smaller exchange constant is only 341.9°. Smaller values of 335.1° are found for cluster (**1**). For cluster (**3**) the coordination geometry around the oxygen bridging the strongly exchange-coupled Cu^{2+}

ions are nearly planar (>350°), whereas for the exchange paths with constants in the region of a few cm^{-1} values between 330° and 340° are obtained. However, the sizes of the exchange constants are not completely determined by geometrical properties. The chemical nature of the bridging alcohol is also very important. For the planar dinuclear Cu^{2+} complex bridged by 3-amino-1-propanol, Matsumoto *et al* [3] determined the large antiferromagnetic exchange constant of $-2J/hc = 920$ cm^{-1} which corresponds well to $J/hc = -450$ cm^{-1} found for the large exchange constant of cluster (**2**). However, for the 3-amino-1-propanol-bridged Cu^{2+} dimer the Cu–O–Cu angle of 103.6° is considerably smaller than 145° determined for cluster (**2**). In order to study these effects, the bridging alcohols of the polyolate clusters should be modified.

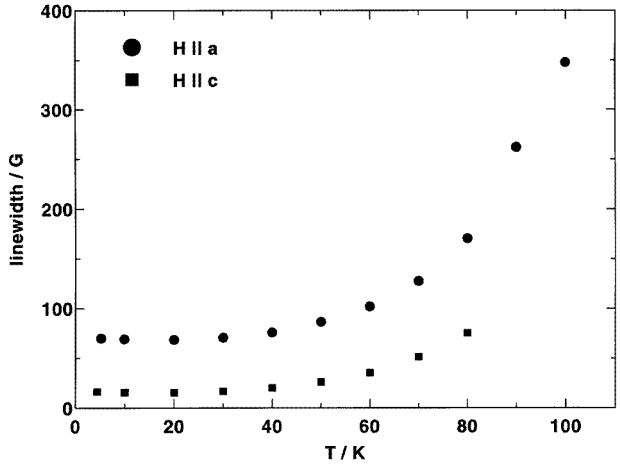

Figure 5. The temperature dependence of the ESR linewidth (peak to peak) at 9.5 GHz.

4. ESR

For all three of the compounds, ESR spectra at 9.5 GHz were recorded between 4.5 K and 300 K. Since the resonance lines of compounds (**1**) and (**3**) are very broad even at low temperatures (4.5 K), no analysis of these spectra was carried out. Figure 5 shows that in the case of compound (**2**) the linewidth decreases drastically with decreasing temperature. Below 80 K there is one well defined Lorentzian-shaped resonance signal which is particularly suitable for a more detailed ESR study. We determined via ESR at 9.5 GHz the spin-Hamiltonian parameters of the of polyolate-bridged Cu^{2+} ions and found proof of the ground-state wavefunction of cluster (**2**). We report also preliminary ESR spectra at 245 GHz, which demonstrate that the single resonance line at 9.5 GHz can be further resolved into several resonance lines, so an ESR study of individual clusters of compound (**2**) becomes possible.

4.1. ESR at 9.5 GHz

For compound (**2**) there are six magnetically inequivalent but crystallographically equivalent clusters. At a frequency of 9.5 GHz it is not possible to resolve the resonances of these six clusters in the unit cell. There is only one exchange-narrowed Lorentzian-shaped resonance

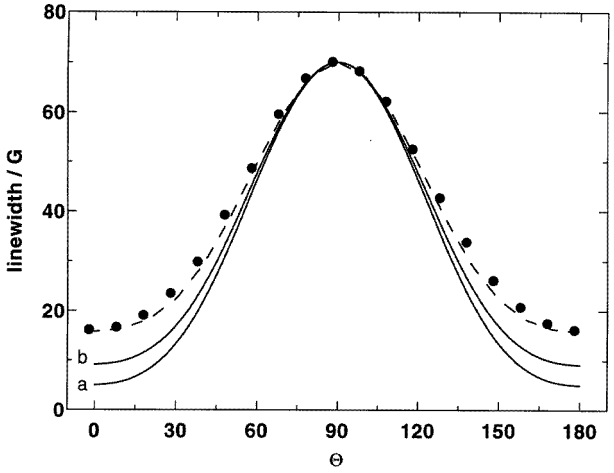

Figure 6. The angular variation of the ESR linewidth (peak to peak) at 9.5 GHz (dots) and 10 K. The solid lines were calculated with $|A_{\parallel}/A_{\perp}| = 5.8$ for the wavefunctions $|A\rangle$ (curve a) and $|B\rangle$ (curve b), respectively. The broken line is for $|A_{\parallel}/A_{\perp}| = 2.9$ and wavefunction $|B\rangle$. For $\Theta = 0$ the magnetic field is applied parallel to the c-axis.

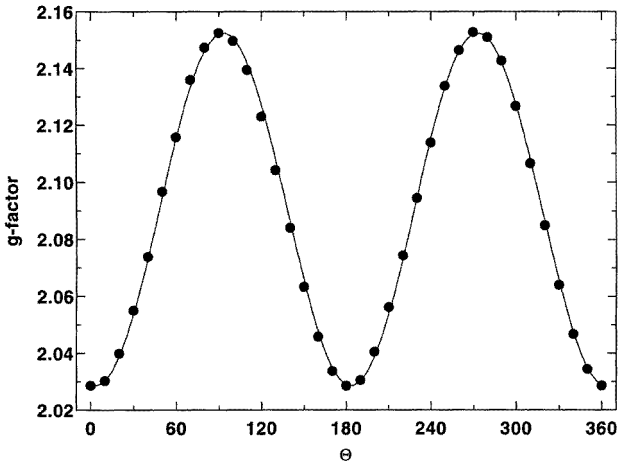

Figure 7. The angular variation of the g-factors at 10 K. Dots: experimental data; solid line: calculated using equation (12). For $\Theta = 0$ the magnetic field is applied parallel to the c-axis.

line, which can be characterized by a linewidth of $\Delta B_{pp} = 18$ G and 65 G, and a g-factor of $g_{\parallel c} = 2.030 \pm 0.003$ and $g_{\perp c} = 2.153 \pm 0.003$, when the magnetic field is applied parallel and perpendicular to the crystallographic c-direction, respectively. Figure 6 displays the angular variation of the linewidth, and figure 7 the angular variation of the g-factor at a temperature of 10 K. At temperatures below 80 K the results are essentially temperature independent.

Similarly to what is found for other polyolate-bridged clusters, there are four oxygen atoms in the nearest neighbourhood of the Cu^{2+} ions. Therefore the ground state of the Cu^{2+} ions is approximately an orbital singlet of $d_{x^2-y^2}$ symmetry. Indeed, the ESR results

obtained at low temperatures can be interpreted at least qualitatively by assuming a pure $d_{x^2-y^2}$-orbital ground state of the Cu^{2+} ions. A $d_{x^2-y^2}$ orbital is characterized by the g-factors $g_\parallel > g_\perp$ and hyperfine constants $|A_\parallel| > |A_\perp|$ [13]. The symbols $\parallel$ and $\perp$ indicate that the magnetic field is applied parallel and perpendicular to the normal of the plane formed by the neighbouring oxygen atoms. When the magnetic field is applied parallel to the c-direction of compound (**2**), the g-factors of all of the Cu^{2+} ions are $g_\perp$, since the normals of the copper oxygen planes are perpendicular to the c-direction (compare figure 1). Therefore the exchange-averaged g-factor has to increase when the magnetic field is turned into the (001) plane. Equally, the linewidth should increase when the magnetic field is turned into the (001) plane—first of all, due to the contribution of the hyperfine interaction to the linewidth, but also due to the anisotropic g-factors of the magnetically different clusters.

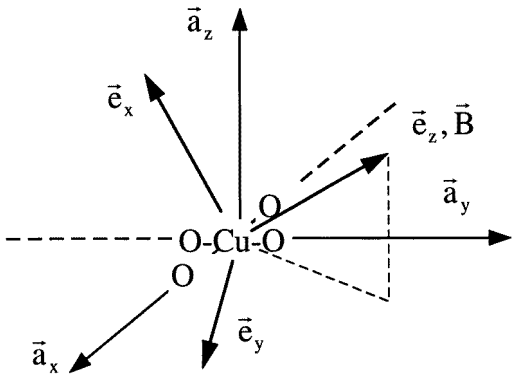

Figure 8. The orientation of the local coordinate systems $\boldsymbol{a}_\nu$ of the Cu^{2+} ions and the common coordinates $\boldsymbol{e}_\mu$ used to describe the whole compound.

A quantitative discussion of the ESR results starts from the wavefunction of three $s = 1/2$ spins, which are antiferromagnetically coupled according to the Hamiltonian of equation (1). The ground-state wavefunction of cluster (**2**) can be characterized by an effective spin $S = 1/2$. Generally, one has

$$\left|S = \frac{1}{2}\right\rangle = \sin\frac{\varphi}{2}|A\rangle + \cos\frac{\varphi}{2}|B\rangle \tag{7}$$

with

$$|A\rangle = \frac{1}{\sqrt{6}}(|+--\rangle + |-+-\rangle - 2|--+\rangle)$$
$$|B\rangle = \frac{1}{\sqrt{2}}(|+--\rangle - |-+-\rangle)$$
$$\cos\varphi = \frac{K}{\lambda}$$

(for K and λ see equation (1) and below). When $J_2 = J_3$ for (**2**), the ground state is given by the wavefunction $|A\rangle$ if $J_1 > 0$, or by wavefunction $|B\rangle$ if $J_1 < 0$. The ground-state properties of the clusters can easily be calculated in terms of the effective spin $S = 1/2$, since the matrix elements of the copper spins $\boldsymbol{s}_i$ are proportional to those of the effective

spin $\boldsymbol{S}$ of the cluster:

$$\begin{aligned} \langle A|\boldsymbol{s}_i|A\rangle &= \rho_i\langle S, m_S|\boldsymbol{S}|S, m_S\rangle \qquad \text{with } \rho_1 = \rho_2 = 2/3 \text{ and } \rho_3 = -1/3 \\ \langle B|\boldsymbol{s}_i|B\rangle &= \rho_i\langle S, m_S|\boldsymbol{S}|S, m_S\rangle \qquad \text{with } \rho_1 = \rho_2 = 0 \text{ and } \rho_3 = 1. \end{aligned} \tag{8}$$

Due to the fourfold symmetry of the nearest neighbourhood of the Cu^{2+} ions (see figure 1(*a*)) an axial spin-Hamiltonian is assumed in order to calculate the properties of the cluster [13, 14]. The ESR spectrum of a frozen solution of the related complex $[Cu(AnErytH_{-2})_2]^{2-}$ [5] confirms the validity of this assumption. The g-factors and hyperfine coupling constants obtained from this spectrum are given in section 4.1.2. It is further assumed that the g-factors and hyperfine constants are the same for all Cu^{2+} ions. Within a local coordinate system $\boldsymbol{a}_\nu$ (see figure 8) of the copper ions one has $g_x = g_y = g_\perp$, $g_z = g_\parallel$ and $A_x = A_y = A_\perp$, $A_z = A_\parallel$. The coordinates $\boldsymbol{e}_\mu$ are used to describe the magnetic resonance of the whole crystal.

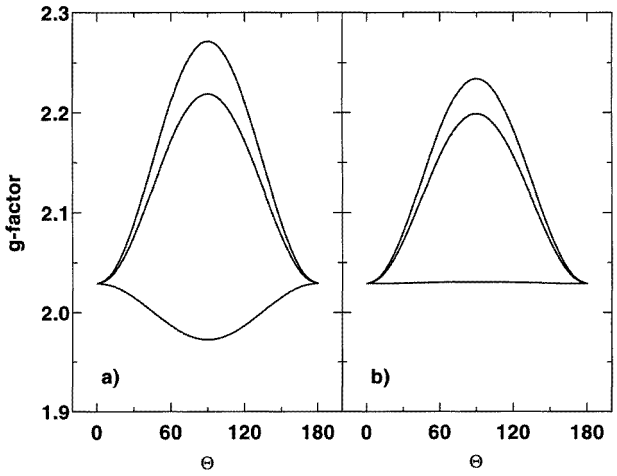

Figure 9. The angular variations of the g-factors of the individual clusters calculated for wavefunctions $|A\rangle$ (a) and $|B\rangle$ (b), respectively. For $\Theta = 0$ the magnetic field is applied parallel to the c-axis.

4.1.1. The g-factor. The Zeeman Hamiltonian for a single Cu^{2+} spin $\boldsymbol{s}_i$ for the system of coordinates $\boldsymbol{a}_\nu$ is

$$H_{Zee} = \sum_{\nu=x,y,z} \mu_B g_\nu B^\nu s_i^\nu \tag{9}$$

and for the system of coordinates $\boldsymbol{e}_\mu$ of the whole crystal one has for the cluster

$$H_{Zee} = \sum_{i=1}^{3} \sum_{\mu=x,y,z} \mu_B g_{z\mu}(i) B^z s_i^\mu \tag{10}$$

with the g-tensor

$$g_{\lambda\mu}(i) = \sum_{\nu=x,y,z} g_\nu(\boldsymbol{e}_\lambda \cdot \boldsymbol{a}_\nu(i))(\boldsymbol{e}_\mu \cdot \boldsymbol{a}_\nu(i))$$

and $\boldsymbol{B} \parallel \boldsymbol{e}_z$. Using the effective spin $\boldsymbol{S}_n$ of cluster n the total Zeeman interaction can be written as

$$H_{Zee} = \sum_n \sum_{\mu=x,y,z} \mu_B g_{z\mu}^{(n)} B^z S_n^\mu. \tag{11}$$

For each of the six magnetically inequivalent clusters, the components of the g-tensor $g_{z\mu}^{(n)}$ of cluster n have to be calculated according to

$$g_{z\mu} = \sum_{i=1}^{3} g_{z\mu}(i)\rho_i.$$

Since only one exchange-averaged resonance line is observed, the g-factor of the line is simply given by the average

$$\bar{g} = \frac{1}{6}\sum_{n=1}^{6} g_{zz}^{(n)} \tag{12}$$

and the mean Zeeman operator is

$$\bar{H}_{Zee} = \sum_n \mu_B \bar{g} B^z S_n^z. \tag{13}$$

The other parts of the Zeeman operator, connected with the g-tensor components $(g_{zz}^{(n)} - \bar{g})$, $g_{zx}^{(n)}$ and $g_{zy}^{(n)}$, contribute to the width of the resonance line (see the next section). The angular variation of the $g_{zz}^{(n)}$ for the individual clusters n depends on the wavefunction of the ground state. Figure 9 displays the angular variation of $g_{zz}^{(n)}$ calculated for the wavefunctions $|A\rangle$ and $|B\rangle$, when the magnetic field is turned within the ac plane. There are three different branches $g_{zz}^{(n)}$, since the clusters are magnetically equivalent in pairs for these directions of the magnetic field. Although the angular variation of the $g_{zz}^{(n)}$ is quite different for the wavefunctions $|A\rangle$ and $|B\rangle$, there is no difference in the averaged $\bar{g}$. Via a comparison of the experimental results (black dots in figure 7) with the angular variation of $\bar{g}$, the g-factors $g_\perp = 2.029 \pm 0.002$ and $g_\parallel = 2.280 \pm 0.002$ for the Cu^{2+} ion are obtained. These values are in good agreement with the known g-factor of Cu^{2+} ions, whose ground states are orbital singlets of $d_{x^2-y^2}$ symmetry [13, 14].

4.1.2. The linewidth. The measurements of the magnetic susceptibility indicate that the intercluster exchange constants $|J/hc|$ are smaller than 0.7 cm^{-1}. Therefore it is justified to restrict the analysis of the linewidth to the secular contributions of the intercluster dipole interaction, the hyperfine interaction of the electrons with the nuclear spins $I = 3/2$ of the copper atoms and those parts of the Zeeman operator not included in the averaged Hamiltonian $\bar{H}_{Zee}$.

The Hamiltonian of the intercluster dipole interaction written in terms of the effective spin $\boldsymbol{S}_n$ of the ground state of the cluster is

$$H_{dipole} = \hbar\frac{1}{4}\omega_d \sum_{n\neq m} A_{nm}^0 (3S_n^z S_m^z - \boldsymbol{S}_n \cdot \boldsymbol{S}_m) \tag{14}$$

with the factors

$$A_{nm}^0 = \sum_{i,j=1}^{3} \left(1 - 3\cos^2(\Theta_{i,j}^{(nm)})\right)\left(\frac{a}{r_{i,j}^{(nm)}}\right)^3 \rho_i \rho_j.$$

Here $r_{i,j}^{(nm)}$ is the distance between the copper atom i on cluster n and the copper atom j on cluster m. Also $\Theta_{i,j}^{(nm)}$ is the angle between the vector $\boldsymbol{r}_{i,j}^{(nm)}$ and the direction of the

applied magnetic field. With the mean distance $a = 5.5$ Å between the clusters one has $\omega_d = (g\mu_B)^2/\hbar a^3 = 1.963 \times 10^9$ rad s^{-1} (104×10^{-4} cm^{-1}).

The secular component of the Zeeman operator contributing to the linewidth is

$$H_{Zee}^{(aniso)} = H_{Zee} - \bar{H}_{Zee} = \sum_n \mu_B B^z (g_{zz}^{(n)} - \bar{g}) S_n^z = \hbar\omega_{Zee} \sum_n \left(\frac{g_{zz}^{(n)} - \bar{g}}{\bar{g}\,\Delta g} \right) S_n^z. \tag{15}$$

$\Delta g = 0.0605$ is a normalization constant, $\omega_{Zee} = \Delta g\, \omega_0 = 3.58 \times 10^9$ rad s^{-1} (190×10^{-4} cm^{-1}) is calculated with the resonance frequency $\omega_0 = 2\pi \times 9.5$ GHz (0.314 cm^{-1}).

The secular part of the hyperfine interaction of the electron with the nuclear spins $I = 3/2$ of the copper atoms is

$$H_{hf} = \hbar\omega_{hf} \sum_n \sum_{i=1}^{3} \sum_{\mu=x,y,z} A_{z\mu}^{(n,i)} \rho_i S_n^z I_i^\mu. \tag{16}$$

The index i runs over the three copper ions of the cluster n, $\omega_{hf} = A_\parallel/\hbar$, and the hyperfine constants are calculated similarly to the components of the g-tensor (equation (9) below):

$$A_{\lambda\mu,i}^{(n)} = \frac{1}{A_\parallel} \sum_{\nu=x,y,z} A_\nu (\boldsymbol{e}_\lambda \cdot \boldsymbol{a}_{\nu,i}^{(n)})(\boldsymbol{e}_\mu \cdot \boldsymbol{a}_{\nu,i}^{(n)}). \tag{17}$$

In order to estimate the magnitudes of the hyperfine constants $A_x = A_y = A_\perp$ and $A_z = A_\parallel$ of the Cu^{2+} ions, a frozen solution of $Na_2[Cu(AnErytH_{-2})_2]$ molecules [5] was analysed. Similarly to what was found for compound (**2**), for $[Cu(AnErytH_{-2})_2]^{2-}$ the nearest neighbourhood of the copper ions is formed by a plane of oxygen atoms, so presumably the hyperfine constants of the two compounds are roughly the same. This assumption is confirmed by the g-factors obtained from the spectrum of the frozen solution: $g_\parallel = 2.23 \pm 0.02$ and $g_\perp = 2.05 \pm 0.02$. The value determined for $|A_\parallel/hc| = (203 \pm 3) \times 10^{-4}$ cm^{-1} agrees well with known hyperfine constants for the $d_{x^2-y^2}$ orbital of Cu^{2+} [15]. However, with $|A_\perp/hc| = (35 \pm 2) \times 10^{-4}$ cm^{-1} the observed ratio $|A_\parallel/A_\perp| = 5.8$ is reduced in comparison with the ratio $|A_\parallel/A_\perp| \approx 15$ expected from the g-factors $g_\perp = 2.03$, $g_\parallel = 2.28$ and a core polarization of $\kappa = 0.32$ for pure Cu^{2+} $d_{x^2-y^2}$ orbitals [15].

The ESR linewidth (half-width at half-height) is given by [16]

$$\Delta B = \frac{1}{\gamma_e} \mathrm{Re} \left\{ \int_0^\infty \mathrm{e}^{-\mathrm{i}\omega t} \langle \mathrm{e}^{\mathrm{i}Ht/\hbar}[H_{ss}, S^+]\mathrm{e}^{-\mathrm{i}Ht/\hbar}[S^-, H_{ss}] \rangle \, \mathrm{d}t \Big/ \hbar^2 \langle S^+ S^- \rangle \right\} \tag{18}$$

with $H_{ss} = H - \bar{H}_{Zee}$. H_{dipole} leads to the four-spin correlation functions

$$f_{ijkl}(t) = \langle s_i^+(t) s_j^+(t) s_k^- s_l^- \rangle / \left[2((2/3)s(s+1))^2 \right]$$

and H_{Zee} and H_{hf} to two-spin correlation functions

$$f_{ij}(t) = \langle s_i^+(t) s_j^- \rangle / ((2/3)s(s+1)).$$

Assuming a short-time Gaussian decay for the correlation functions due to the intercluster exchange interaction

$$H_{inter} = J \sum_{i \neq j \in \{n.n.\}} \boldsymbol{s}_i \cdot \boldsymbol{s}_j$$

($f_{ijkl} = \delta_{ik}\delta_{jl}\mathrm{e}^{-2zJ^2t^2/\hbar^2}$ and $f_{ij} = \delta_{ij}\mathrm{e}^{-zJ^2t^2/\hbar^2}$) the Fourier transforms of the correlation functions are

$$\tilde{f}_{ijkl}(\omega) = \int_{-\infty}^{\infty} f_{ijkl}(t)\mathrm{e}^{-\mathrm{i}\omega t} \, \mathrm{d}t = \delta_{ik}\delta_{jl} \sqrt{\frac{\pi}{2z(J/\hbar)^2}} \exp\left[-\frac{1}{8z} \left(\frac{\omega}{J/\hbar} \right)^2 \right]$$

$$\tilde{f}_{ij}(\omega) = \int_{-\infty}^{\infty} f_{ij}(t)\mathrm{e}^{-\mathrm{i}\omega t} \, \mathrm{d}t = \delta_{ij} \sqrt{\frac{\pi}{z(J/\hbar)^2}} \exp\left[-\frac{1}{4z} \left(\frac{\omega}{J/\hbar} \right)^2 \right].$$

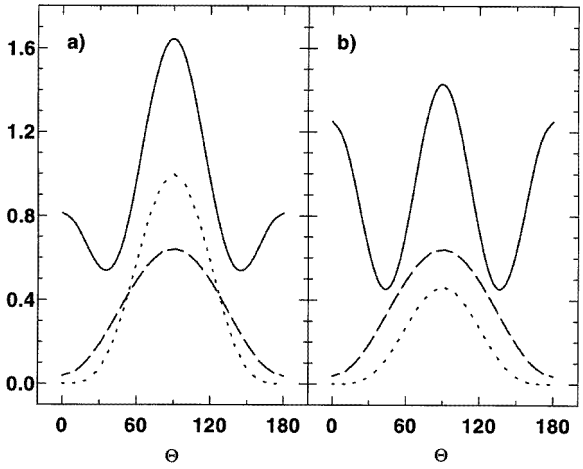

Figure 10. The expected angular variation of the dipolar (solid line), Zeeman (dotted line) and hyperfine contributions (dashed line) to the ESR linewidth, calculated for the wavefunctions $|A\rangle$ (a) and $|B\rangle$ (b), respectively. For $\Theta = 0$ the magnetic field is applied parallel to the c-axis.

z is the number of the nearest neighbours of the clusters. Assuming further that $|\sqrt{z}J/\hbar| \ll \omega_0$, the dipolar contribution to the exchange-narrowed linewidth is given by ($\gamma_e = 1.76\times10^7$ rad s^{-1} G^{-1})

$$\Delta B_{dipole} = \frac{1}{\gamma_e}\sqrt{\frac{\pi}{2}}\frac{3s(s+1)}{8}\frac{\omega_d^2}{|\sqrt{z}J/\hbar|}\frac{1}{N}\sum_{i\neq j}|A_{ij}^0|^2 = \frac{0.41\ (\mathrm{cm}^{-1}\ \mathrm{G})}{|\sqrt{z}J/hc|}\frac{1}{N}\sum_{i\neq j}|A_{ij}^0|^2. \qquad (19)$$

The Zeeman contribution is given by

$$\Delta B_{Zee} = \frac{1}{\gamma_e}\frac{\sqrt{\pi}}{2}\frac{\omega_{Zee}^2}{|\sqrt{z}J/\hbar|}\frac{1}{N}\sum_i\left(\frac{g_{zz}^{(i)}-\bar{g}}{\bar{g}\,\Delta g}\right)^2 = \frac{3.42\ (\mathrm{cm}^{-1}\mathrm{G})}{|\sqrt{z}J/hc|}\frac{1}{N}\sum_i\left(\frac{g_{zz}^{(i)}-\bar{g}}{\bar{g}\,\Delta g}\right)^2 \qquad (20)$$

and the hyperfine contribution by

$$\Delta B_{hf} = \frac{1}{\gamma_e}\frac{\sqrt{\pi}}{2}\frac{\omega_{hf}^2}{|\sqrt{z}J/\hbar|}\frac{I(I+1)}{3}\frac{1}{N}\sum_n\sum_{\mu=x,y,z}\sum_{i=1}^{3}(A_{z\mu,i}^{(n)}\rho_i)^2$$
$$= \frac{4.9\ (\mathrm{cm}^{-1}\ \mathrm{G})}{|\sqrt{z}J/hc|}\frac{1}{N}\sum_n\sum_{\mu=x,y,z}\sum_{i=1}^{3}(A_{z\mu,i}^{(n)}\rho_i)^2. \qquad (21)$$

Figure 10 displays the angular variation within the ac plane of

$$\frac{1}{N}\sum_{i\neq j}|A_{ij}^0|^2 \qquad \frac{1}{N}\sum_i\left(\frac{g_{zz}^{(i)}-\bar{g}}{\bar{g}\,\Delta g}\right)^2 \qquad \frac{1}{N}\sum_n\sum_{\mu=x,y,z}\sum_{i=1}^{3}(A_{z\mu,i}^{(n)}\rho_i)^2$$

calculated for the wavefunctions $|A\rangle$ and $|B\rangle$, respectively. For the two wavefunctions one gets the same variation of the hyperfine contribution. The Zeeman contribution is larger by a factor of two for wavefunction $|A\rangle$ than for $|B\rangle$, when the magnetic field is applied perpendicular to the c-direction. Hyperfine and Zeeman contributions dominate the angular variation of the linewidth. The dipolar contribution is only important when the magnetic field is applied parallel to the c-direction. Its angular variation strongly depends on the distribution of the spin density over the cluster.

A comparison between the experimental results and the linewidth calculated according to equations (19)–(21) is shown in figure 6. The difference between the calculations carried out for wavefunctions $|A\rangle$ and $|B\rangle$ is considerably smaller than might be expected from figure 10, since the maxima of the calculations are adjusted by the intercluster exchange constants to the experimental data. The values $|\sqrt{z}J/hc| = 0.119$ cm^{-1} and 0.087 cm^{-1} are used for $|A\rangle$ and $|B\rangle$, respectively. With the ratio $|A_\parallel/A_\perp| \approx 5.8$, determined from the frozen solution of $Na_2[Cu(AnErytH_{-2})_2]$, a slightly better result is found for the wavefunction $|B\rangle$ than for $|A\rangle$. This confirms the negative value of the exchange constant J_1 which was obtained by comparing the magnetic susceptibilities of clusters (**1**) and (**2**). The fit of the experimental data can be improved by decreasing the ratio $|A_\parallel/A_\perp|$ and keeping $A_\parallel$ constant. The dashed line of figure 6 is obtained for a ratio $|A_\parallel/A_\perp| = 2.9$ ($|\sqrt{z}J/hc| = 0.093$ cm^{-1} for wavefunction $|B\rangle$), which is considerably smaller than the ratio expected for a pure $d_{x^2-y^2}$ orbital of the copper ions.

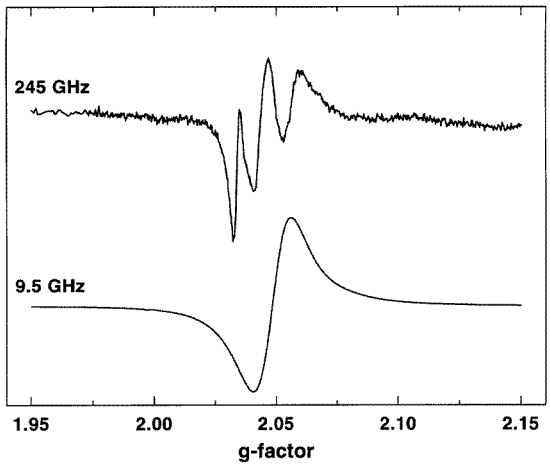

Figure 11. A comparison between the resonance signals at 20 K obtained at 9.5 GHz and 245 GHz. The magnetic field was applied at about 30° with respect to the *c*-direction.

4.2. ESR at 245 GHz

If there is exchange narrowing of different ESR resonances, the minimal resolvable difference between the *g*-factors of two resonances is approximately given by $\Delta g/g \approx |\sqrt{z}J|/h\nu$. Due to the intercluster exchange interaction $|\sqrt{z}J/hc| \simeq 0.1$–$0.2$ cm^{-1}, the resonance signals of the individual clusters of compound (**2**) cannot be resolved at 9.5 GHz, since the minimal resolvable $\Delta g/g$ is in the region of 0.5. However, at 245 GHz the minimal value of $\Delta g/g \simeq 0.02$ is considerably smaller, so a more accurate determination of the *g*-factors and hyperfine coupling constants becomes possible from an investigation of the resonance lines which correspond to individual clusters. The increase of resolution obtained at a frequency of 245 GHz is shown in figure 11. This figure compares the resonance signals observed at 9.5 GHz and 245 GHz, when a magnetic field is applied at 30° with respect to the *c*-direction. The single resonance at 9.5 GHz can be resolved into three lines at 245 GHz. In order to obtain quantitative results taking angle-dependent measurements on well oriented crystals is necessary. This was not possible. However, preliminary angle-dependent measurements carried out at 20 K demonstrate directly that

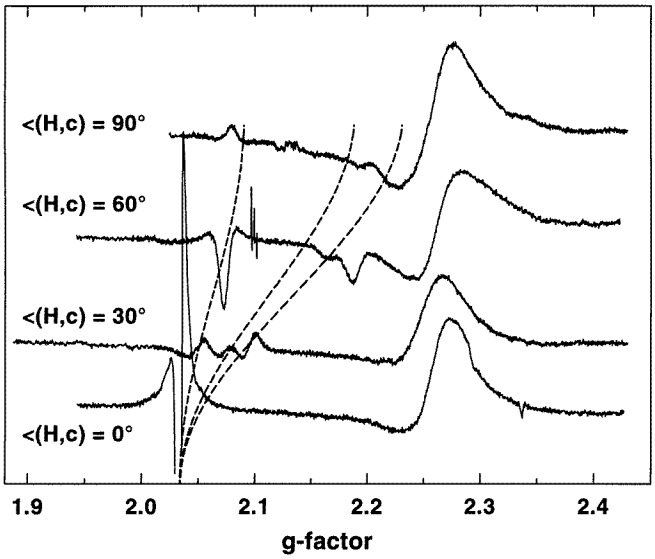

Figure 12. The angular variation of the resonance signals at 20 K for a frequency of 245 GHz.

the ground state of cluster (**2**) is given by the wavefunction $|B\rangle$. Figure 12 shows the measurement for different angles of the magnetic field with respect to the c-axis. Similarly to what is found for the measurements at 9.5 GHz, there is one strong resonance for $\boldsymbol{B}\|\boldsymbol{c}$. For magnetic fields applied at 30°, 60° and 90° with respect to the c-axis, three weak resonances can be resolved. The dashed lines of figure 12 are guides to the eye, in order to show clearly the shifts of the resonances. Roughly, the lines follow the angular variation of the g-factors expected for wavefunction $|B\rangle$ (see figure 9(b)). However, more detailed investigations would be necessary in order to obtain quantitative results.

Additionally to the expected resonance lines, there is a resonance at $g = 2.25$ for 245 GHz. Since there is no obvious reason for a zero-field splitting of the electronic states of compound (**2**), the unknown resonance may stem from oxygen present in the sample chamber.

5. Conclusion

The magnetic properties of the polyolate-bridged clusters of $Li_3[Cu_3(\mu\text{-}C_3H_5O_3)_3]\cdot 18H_2O$ (**1**), $Na_3[Cu_3(\mu\text{-}C_3H_5O_3)_3]\cdot 9H_2O$ (**2**) and $Li_8[Cu_{16}(C_6H_8O_6)_4(C_6H_{10}O_6)_4]\cdot 44H_2O$ (**3**) are determined by a strong antiferromagnetic exchange interaction between the Cu^{2+} ions of the clusters. By measuring the static magnetic susceptibility, we obtained the Cu–O–Cu exchange constants for different Cu–O–Cu angles. The clusters of compound (**1**) have a threefold symmetry axis, so the intracluster exchange interaction of $J/hc = -42$ cm^{-1} is the same for interactions between all of the Cu^{2+} ions ($\angle$(Cu–O–Cu) $\simeq$ 120°). For the clusters of compound (**2**) (point symmetry C_s), there are two different exchange constants: $J/hc = -450$ cm^{-1} for $\angle$(Cu–O–Cu) $\simeq$ 140° and $J/hc = -42$ cm^{-1} for $\angle$(Cu–O–Cu) $\simeq$ 120°. Measurements of the magnetic susceptibility of compound (**3**) show that this cluster of 16 copper ions consists of four groups of strongly antiferromagnetically coupled Cu^{2+} ions. The resulting spins of these four groups are only weakly exchange

coupled. Since the four spin groups are mutually linked by Cu–O–Cu bonds with angles in the range between 110° and 115°, the weak exchange interaction between them indicates that the character of the exchange interaction changes in this range of Cu–O–Cu angles from antiferromagnetic to ferromagnetic interaction.

A detailed ESR study was carried out for compound (**2**). At 9.5 GHz, there is one Lorentzian-shaped resonance at temperatures below 80 K. The linewidth and g-factor of the resonance are mainly determined by the g-anisotropy, the hyperfine interaction of the Cu^{2+} ions, and their strong antiferromagnetic intracluster coupling. The magnetic dipole interaction between different clusters is of minor importance. The g-factors obtained for the Cu^{2+} ions ($g_\perp = 2.03$ and $g_\parallel = 2.28$) confirm that the ground state is mainly an orbital singlet of $d_{x^2-y^2}$ symmetry pointing towards the four neighbouring oxygen atoms. The hyperfine constant $|A_\parallel/hc| = 203 \times 10^{-4}$ cm^{-1} is also in good agreement with the values usually obtained for $d_{x^2-y^2}$ orbitals of Cu^{2+} ions. However, the ratio $|A_\parallel/A_\perp| = 2.9$ is smaller than expected and indicates orbital contributions of the ligands to the $d_{x^2-y^2}$ orbital.

Preliminary measurements at 245 GHz of compound (**2**) show that it is possible to overcome the averaging effect of the intercluster exchange interaction. The angular variation of the resonance-field strengths of individual clusters can be observed and confirm independently the intracluster exchange constants determined by magnetic susceptibility measurements. Better measurements of carefully oriented samples are necessary in order to determine from the angular variation of the resonance fields and the linewidths the g-factors and hyperfine constants.

Acknowledgments

The authors would like to thank Professor E Dormann for stimulating discussions, H Winter for measuring the magnetic susceptibility and W Palme for technical assistance during the ESR measurements at 245 GHz. Part of the work was carried out in the ESR group of J P Boucher at the Laboratoire Des Champs Magnétiques Intenses in Grenoble and was supported by the Human Capital and Mobility Programme of the European Community.

References

[1] Van Crawford H, Richardson H W, Wasson J R, Hodgson D J and Hatfield W E 1979 *Inorg. Chem.* **15** 2107
[2] Schawabe L and Haase W 1985 *J. Chem. Soc. Dalton Trans.* 1909
[3] Matsumoto N, Tsutsumi T, Ohyoshi A and Okawa H 1983 *Bull. Chem. Soc. Japan* **56** 1388
[4] Mikuriya M, Okawa H and Kida S 1982 *Bull. Chem. Soc. Japan* **55** 1086
[5] Klaassen M and Klüfers P 1993 *Z. Anorg. Allg. Chem.* **619** 661
[6] Klüfers P and Schuhmacher J 1994 *Angew. Chem.* **106** 1839
[7] Klüfers P and Schuhmacher J 1995 unpublished
[8] Klüfers P and Schuhmacher J 1995 *Angew. Chem.* **107** 2290
[9] Muller F, Hopkins M A, Coron N, Grynberg M, Brunel L C and Martinez G 1989 *Rev. Sci. Instrum.* **60** 3681
[10] Haberditzl W 1968 *Magnetochemie* (Berlin: Akademie)
[11] 1967 *Magnetic Properties II; Landolt–Börnstein* vol 10 (Berlin: Springer) p 21 (χ_{Dia} of water), p 74 (χ_{Dia} of glycerol)
[12] de Jongh L J 1988 *Solid State Commun.* **65** 963
[13] Abragam A and Bleaney B 1970 *Electron Paramagnetic Resonance of Transition Ions* (Oxford: Clarendon)
[14] Hoffmann S K, Geher M A S, Hilczer W, Goslar J and Hafez A K 1994 *Acta Phys. Pol.* A **85** 517
[15] See table 7.22 in [13].
[16] Boucher J P, Ahmed Bakheit M, Nechtschein M, Villa M, Bonera G and Borsa F 1976 *Phys. Rev.* B **13** 4098